ACS APPLIED MATERIALS & INTERFACES

Research Article

www.acsami.org

Study of Factors Governing Oil–Water Separation Process Using TiO_2 Films Prepared by Spray Deposition of Nanoparticle Dispersions

Mohammed A. Gondal,*[,†] Muhammad S. Sadullah,[†] Mohamed A. Dastageer,[†] Gareth H. McKinley,[‡] Divya Panchanathan,[‡] and Kripa K. Varanasi[‡]

[†]Laser Research Group, Physics Department and Center of Excellence in Nanotechnology (CENT), King Fahd University of Petroleum & Minerals, Dhahran 31261, Saudi Arabia

[‡]Department of Mechanical Engineering, Massachusetts Institute of Technology, Cambridge, Massachusetts 02139-4307, United Sates

Supporting Information

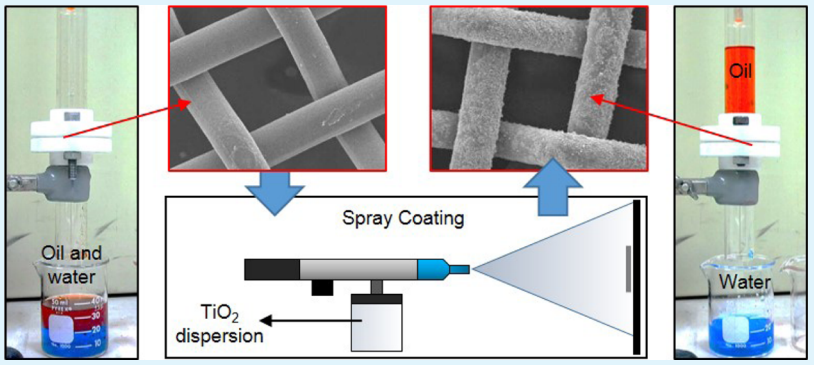

ABSTRACT: Surfaces which possess extraordinary water attraction or repellency depend on surface energy, surface chemistry, and nano- and microscale surface roughness. Synergistic superhydrophilic-underwater superoleophobic surfaces were fabricated by spray deposition of nanostructured TiO_2 on stainless steel mesh substrates. The coated meshes were then used to study gravity driven oil–water separation, where only the water from the oil–water mixture is allowed to permeate through the mesh. Oil–water separation efficiencies of up to 99% could be achieved through the coated mesh of pore sizes 50 and 100 μm, compared to no separation at all, that was observed in the case of uncoated meshes of the same material and pore sizes. An adsorbed water on the TiO_2 coated surface, formation of a water-film between the wires that form the mesh and the underwater superoleophobicity of the structured surface are the key factors that contribute to the enhanced efficiency observed in oil–water separation. The nature of the oil–water separation process using this coated mesh (in which the mesh allows water to pass through the porous structure but resists wetting by the oil phase) minimizes the fouling of mesh so that the need for frequent replacement of the separating medium is reduced. The fabrication approach presented here can be applied for coating large surface areas and to develop a large-scale oil–water separation facility for oil-field applications and petroleum industries.

KEYWORDS: *oil–water separation, superhydrophilicity, underwater superoleophobicity, textured surface, titania*

INTRODUCTION

Petrochemical industries and environmental protection agencies are facing huge technological challenge in developing effective methods for oil–water separation in produced water treatment. Large volumes of water are injected into aging oil wells in order to recover the maximum amount of oil, and this leads to the production of huge amounts of oil–water mixture (or "produced water").[1,2] As this produced water is considered environmentally hazardous, oil producers are now legally bound to recycle the produced water.[3,4] Every year, millions of barrels of crude oil and refined petroleum products are spilled into the seas by tankers, offshore platforms, drilling rigs and oil cargo ships,[5] causing extensive damage to marine ecosystems. An effective oil–water separation method will be beneficial to the ever growing need for oil slick cleanup operations. Many oil–water separation methods like adhesion, gravity separation, absorbance, membrane filtration, and chemical and biological treatments have been developed over the years and most of these techniques are widely used. However, achieving an oil–water separator with low power consumption and high separation efficiency is still a great challenge.[6] Since immiscible oil–water mixtures are governed by interfacial phenomenon, an effective method for the separation can be provided by selecting or synthesizing a material with preferential wetting toward oil or water. For materials that are hydrophobic–oleophilic materials, the water contact angle (denoted θ_{wa}) is greater

Received: March 30, 2014
Accepted: July 24, 2014
Published: July 24, 2014

than 90° and the oil contact angle (θ_{oa}) is less than 90°, and this makes filters constructed from such materials nonwettable by water and wettable by oil. When hydrophobic-oleophilic materials are used as the oil pass filters in oil−water separation, they easily get fouled by viscous oil residues and hence cannot be used for large scale separation methods.[7−10] Other possible materials with different wetting characteristics that can be used on the mesh for gravity driven oil−water separation are of hydrophilic−oleophobic (θ_{wa} < 90° and θ_{oa} > 90°) and superhydrophilic-superoleophobic (θ_{wa} < 5° and θ_{oa} > 150°) character.[11]

The two most prominent membrane filtering techniques employed for oil−water separation are gravity driven and cross-flow filtration. Of these two methods, the gravity driven method is preferred due to the much lower cost and higher permeate collection rate, compared to cumbersome and expensive cross-flow filtration systems.[12,13] The ideal filter surface for gravity-driven filtration is a counterintuitive hydrophilic-oleophobic structure or the more efficient superhydrophilic-superoleophobic surfaces. Since the surface tension of water is greater than that of oil, materials with this kind of wettability are technically more difficult to fabricate and this mechanism often involves superomniphobic materials (θ_{wa} and θ_{oa} > 150°), which can respond to external triggers to generate the superhydrophilicity.[14−16] Kota et al.[16] reported hygroresponsive superhydrophilic−superoleophobic surfaces on meshes and fabrics, coated with fluorodecyl polyhedral oligomeric silsesquioxane (fluorodecyl POSS) blended with poly(ethylene glycol) diacrylate (PEGDA). Fluorodecyl POSS has a very low surface energy ($\gamma_{sv} \approx 10$ mN/m), and hence it has been used in the construction of many liquid repellent surfaces.[17] However, fluorodecyl POSS is quite expensive, and in pure form it has a poor adherence to the underlying substrate. Cao et al. reported oil repellency behavior on porous silicon film.[18] Zhang et al.[19] demonstrated superoleophobic surfaces on perfluorosilane-rendered titania (TiO_2)/single-walled carbon nanotube composite coatings, and upon further UV irradiation, these surfaces passed from the Cassie[20] to the Wenzel state[21] and finally to the inverse Cassie regime.[19]

Oil−water separation can also be achieved using superhydrophilic materials that possess underwater superoleophobicity, i.e., the respective contact angles are θ_{wa} < 5° and θ_{ow} > 150°. In addition to this, photoinduced oil−water separation and self-cleaning ability from fouling have also been demonstrated to be important in the separation performance.[22,23,25] Various preparation methods such as layer-by-layer coating, polymerization, sol gel method, hydrothermal treatments, direct oxidation, and chemical vapor deposition have been employed, and various materials such as hydrogel, silicate, TiO_2, silica gel, zeolite, and nanostructured ZnO surfaces have been studied in order to achieve superhydrophilic surface with good underwater−oil repellency.[22−27] However, most of these preparation methods involve multiple processes, long and delicate methods of sample preparation, exotic materials, and extreme physical conditions to achieve a surface with such wetting properties.

In the case of cold spray coating method, the coating application is carried out at ambient temperatures that are much lower than the melting point of the substrate material. Consequently undesirable thermal factors like oxidation, thermal degradation, and unwanted formation of defects on the coated surface can be minimized. Also in the cold spray coating, the deposited material is accelerated at very high velocity with the help of compressed gas and this can enable spray droplets to undergo an extreme and rapid plastic deformation on impact, thereby, compressing and conformally coating a layer of material on the substrate. Because of the large generation of interfacial area and the rapid drying of the volatile carrier/solvent, the sprayed deposits are typically rough or nonuniform in texture. Because surface roughness is one of the major factors controlling the hydrophilicity of the surface, with this cold spray deposition method, the surface roughnesses of the resulting films can be tuned by controlling the amount of deposited TiO_2 nanoparticles on the mesh.

In the present study, we fabricated superhydrophilic surfaces that exhibit underwater superoleophobicity by the spray coating of nanostructured TiO_2 on stainless steel mesh. This method of fabrication is not only rapid, simple, and cost-effective but also the coated mesh shows an excellent water affinity and strong underwater−oil repellency. The coated meshes are characterized by SEM, XRD, and contact angle goniometry. The superhydrophilic and underwater superoleophobic TiO_2 coated mesh was used for the gravity-driven oil−water separation experiments and showed 99% oil−water separation efficiency by letting water pass through the mesh and retaining the oil above the mesh. The adsorbed layer of water on the coated surface, formation of a water-film between the individual wires of the mesh, and the strength of the underwater superoleophobicity all contribute to this enhanced efficiency of oil−water separation.

EXPERIMENTAL SECTION

TiO_2 films on the stainless steel mesh were fabricated using spray coating with fine nanoparticle dispersions.[28,29] The TiO_2 used in this work is in the anatase phase with an average particle size <25 nm, 99.7% trace metal basis (TEM image in Figure S1). It has a surface area of 60 m^2/gram and a density of 4.26 g/mL (Sigma-Aldrich, CAS 1317-70-0). The stainless steel mesh substrates of different pore sizes were purchased from TWP Inc., USA. Prior to the spray coating, the substrates were cleaned with acetone, isopropanol, and deionized (DI) water and then dried. The spray coating was carried out inside a fume hood with a spray gun (McMaster Carr) of 0.75 mm nozzle diameter using a nitrogen pressure source with an application pressure of 170 kPa. The substrate/mesh was kept at a distance of 20 cm away from the nozzle and the diameter of the coated circular area was between 7 and 10 cm (illustrated in Figure S2 of the Supporting Information).

The TiO_2 dispersion was prepared by adding 0.1 g of TiO_2 nanoparticles in 10 mL of tetrahydrofuran (THF) and sonicating the mixture for 1 h in order to create a stable suspension. The TiO_2 nano dispersion in THF was observed to be visually stable, and no significant precipitation was found even 3 h after preparation. In order to experimentally confirm the stability of the suspension, the monochromatic absorbance of the suspension at 350 nm (the wavelength at which the dispersion shows the absorbance maximum) with respect to time was monitored. It was found that there was no significant change in the absorbance after 3 h. For every coating, a fresh dispersion was prepared and used immediately after sonication. Other solvents such as acetone, isopropanol (IPA), ethanol, and methanol were also tried but only THF and IPA were found to create a stable dispersion of TiO_2. THF was ultimately selected for the spray coating process because it has a lower boiling point (66 °C) which enabled faster evaporation. After deposition, the samples were annealed in air at 550 °C for 2 h.

The scanning electron microscope images were taken using Jeol JSM-6610LV, under 15 kV operating voltage and the X-ray diffractogram (XRD) was taken using Bruker D8−40 kV/40 mA X-ray diffractometer. Contact angles were measured using a Krüss easy drop DSA20X goniometer. All contact angles and the sliding angles were measured five times and the values presented are the averages of

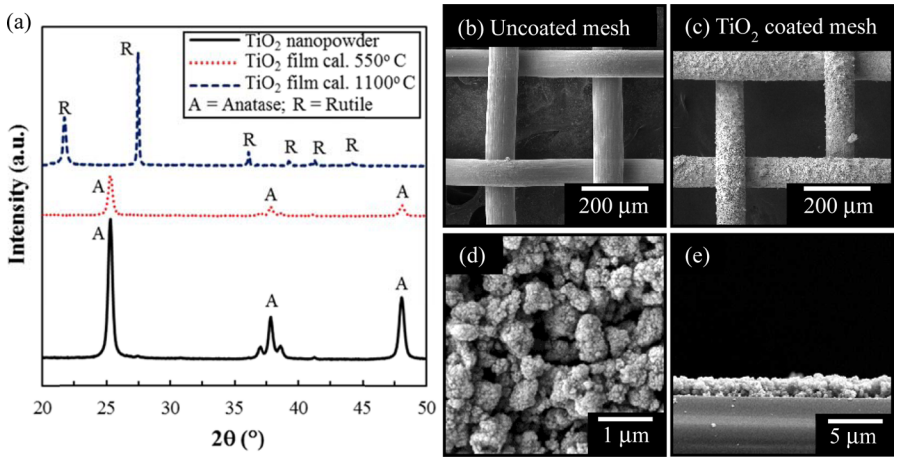

Figure 1. Surface characterization of TiO_2 coated samples. (a) XRD patterns of TiO_2 nanopowder and TiO_2 films calcined at 550 and at 1100 °C. SEM images of (b) uncoated stainless steel mesh and TiO_2 coated stainless steel mesh at (c) low and (d) high magnification, and (e) a cross sectional view.

these values. The oil−water separation system was custom designed and locally fabricated. The system consists of two pieces of Pyrex tubes of 1.7 cm diameter, coupled together with a Teflon flange and oil resistant O rings, which also hold the coated mesh between the two tubes. The coated mesh was wetted with water before inserting it in the oil−water separation module.

RESULTS

Generally metals, alloys, metal oxides, and the oxides of semiconductors naturally exhibit superhydrophilicity due to their large surface energies. In this work, we selected nano titania (TiO_2) in its anatase phase for the fabrication of superhydrophilic surface, because this material is stable, inexpensive, and photocatalytic in nature, in addition to exhibiting remarkable superhydrophilicity. In order to study the effect of annealing on the spray coated titania textures, the TiO_2 films sprayed onto glass substrates were annealed at two different temperatures (550 and 1100 °C) for 2 h, and it was found that the annealing made the TiO_2 surface mechanically more robust. However, annealing at 1100 °C also brought about an undesirable phase transformation from anatase to rutile phase, which is evident from the XRD patterns presented in Figure 1a. This phase transformation of TiO_2 to rutile phase, triggered by high temperature annealing is not desired, because the metastable anatase TiO_2 has larger surface area and greater photocatalytic activity,[30] which can be potentially used in the future for light actuated advanced applications.[15,16,31] The only benefit of annealing the TiO_2 film at the higher temperature is to make the surface mechanically more robust, and hence, all the TiO_2 coated surfaces presented in this work were annealed at 550 °C.

SEM images of the uncoated stainless steel mesh surface and comparable images of TiO_2 spray coated stainless steel mesh surface are depicted in Figure 1b,c, respectively. The smooth uncoated surface having a pore size of approximately 250 μm is shown in Figure 1b and it is clear from Figure 1c that after coating the mesh is uniformly covered with a TiO_2 nanoparticle layer. A higher resolution SEM depicted in Figure 1d indicates that this mesh has both micro and nanoscale surface roughness and this surface roughness is crucial for controlling surface wettability.[20,21] The cross sectional view of the film depicted in Figure 1e shows that the layer thickness is approximately 3 μm.

We also carried out contact angle and sliding angle measurements to characterize the wetting properties of the different fabricated surfaces and these are shown in Figure 2.

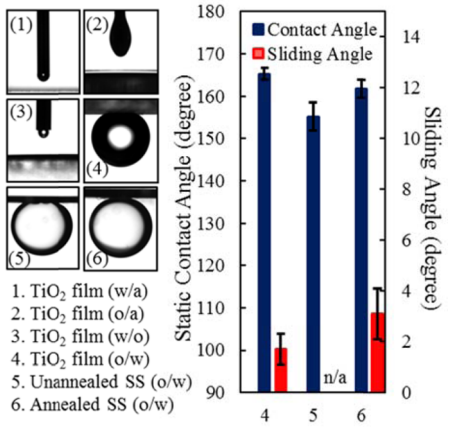

Figure 2. Contact angle and sliding angle measurements for different surfaces (samples 1−6) Except for sample 5, all the samples were annealed. SS stands for stainless steel. Images 1−4 shows that TiO_2 films are superhydrophilic and superoleophilic in air environment and superoleophobic in water environment. Sliding angle was not observed on unannealed stainless steel (sample 5). Superoleophobicity was also achieved on annealed stainless steel (sample 6) even without TiO_2 nanoparticle coating.

The images numbered 1, 2, and 3 on the left part of Figure 2 depict the contact angles of water in air (w/a), oil in air (o/a), and water in oil (w/o) for the TiO_2 coated glass surfaces. For all the above three (images 1−3), the measured contact angles are close to zero (θ_{wa}, θ_{oa}, and $\theta_{wo} \approx 0$) indicating strong wettability. The images 4, 5, and 6 on the left part of Figure 2 show the shape of an oil droplet in water (o/w) for TiO_2 coated glass surface, unannealed stainless steel substrate (uncoated), and annealed stainless steel substrate (uncoated), respectively. For all three cases (images 4−6) the contact angles are more than 150 degrees ($\theta_{ow} > 150°$) and hence these three surfaces are superoleophobic underwater. The contact angles of oil in water for the three surfaces shown in images 4−6 are very close to one another but they may be differentiated in terms of their oil wettability by measuring their oil in water sliding

angles, which are depicted in the bar charts on the right part of Figure 2. For TiO_2 coated glass (bar chart, 4), the oil droplet starts sliding at 1.7 ± 0.5°, whereas the same measurement for the annealed stainless steel substrate (bar chart- 6) gives a sliding angle of 3.1 ± 1.0°. However, for the unannealed stainless steel substrate (bar chart, 5), no sliding was observed. From these contact angle and sliding angle measurements, it is quite evident that the annealed stainless steel mesh (uncoated) exhibits underwater superoleophobicity. The small differences in the measured sliding angle could be due to the oxidation state of the metallic surface as a result of annealing at 550 °C in air environment. This oxidation helps to promote the formation of hydrogen bonds and consequently enhances the surface hydrophilicity and underwater oleophobicity.[32,33]

However, it will be clear from the subsequent discussions that underwater−oil repellency of the mesh is just a necessary, but not sufficient, condition for a mesh to be a good filtering medium for oil−water separation. Even when the oil is in contact with TiO_2 surface, a small volume of water can easily displace the oil in the porous surface of the coating, resulting in a contact angle of water droplets in oil of $\theta_{ow} \rightarrow 0°$ as shown in Figure 2 (image 3). The following test was performed to confirm that a water film replaces the oil that is imbibed into the porous coating. The TiO_2 coated glass slide was immersed in hexadecane and on this surface, a water droplet with an approximate volume of $V = 6 \pm 1$ μL was placed. The water/oil (or w/o) contact angle was measured and found to be $\theta_{ow} = 0°$. This result confirms that water perfectly wets the TiO_2 coated surface even in an oil environment (hexadecane) and also that water replaces the oil trapped in the porous surface. This result is important because water needs to be channeled through the mesh while retaining the oil in the process of oil−water separation using TiO_2 coated stainless steel mesh.

Prior to the actual application and study of oil−water separation using a TiO_2 coated mesh, we demonstrate the underwater superoleophobicity of the TiO_2 coated mesh shown in Figure 3. We carried out oil in water contact angle (θ_{ow}) measurements using different alkanes for TiO_2 coated and uncoated stainless steel meshes and compared the results with a flat TiO_2 coated glass substrate. It should be noted that the TiO_2 coated mesh and TiO_2 coated glass discussed in Figure 3 were annealed, whereas the uncoated mesh was not annealed.

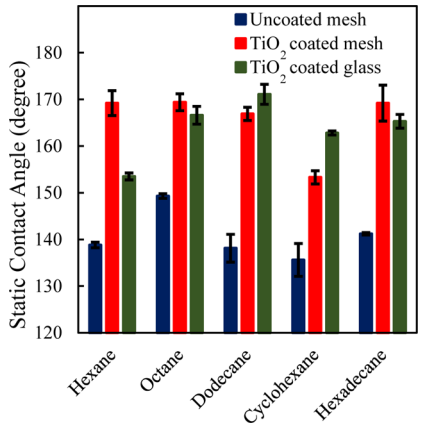

Figure 3. Contact angle measurement of oil drops immersed in a water environment. Different alkanes were tested on an uncoated mesh (blue), TiO_2 coated mesh (red), and a flat TiO_2 coated glass substrate (green).

Figure 3 compares the values of θ_{ow} measured for five different oils on three different surfaces, mentioned above, and it is evident that the TiO_2 coating significantly improves the oil repellency of the stainless steel mesh invariably for all the oil samples under study. The average value of θ_{ow} for the oil samples listed above on a TiO_2 coated stainless steel mesh is 164 ± 6°, which is comparable with the oil in water contact angle of TiO_2 coated glass substrate for the same oil samples under study. Also the sliding angle for the TiO_2 coated mesh is very small while for the uncoated mesh, surface pinning dominates and no sliding angle could be observed even for 30° inclination (see Figure S3).

Pictorial views of the oil−water separation system developed for this study are shown in Figure 4, along with SEM images of

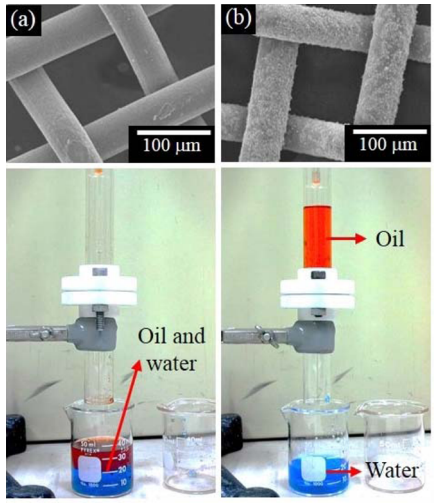

Figure 4. Oil−water separation setup facility developed in our laboratory. Photograph of separation result using (a) annealed uncoated stainless steel mesh and (b) TiO_2 coated stainless steel mesh with the same pore size (100 μm).

coated and uncoated stainless steel meshes with 100 μm pore sizes. The oil−water mixture is poured into the top glass tube, and the permeate is collected in a beaker placed underneath the bottom tube. In order to understand the critical role of TiO_2 coating on the stainless steel mesh, we first used a thermally annealed but uncoated stainless steel mesh in between the glass tubes and found that both the oil and water permeated rapidly through the mesh as exhibited in Figure 4a. On the other hand, when TiO_2 coated stainless steel mesh was used in between the two tubes, the water in the oil−water mixture permeated through the coated mesh leaving the oil in the top glass tube as shown in Figure 4b.

In this oil−water separation system, we used TiO_2 coated stainless steel meshes of four different pore sizes and tested three different oil−water mixture samples. The volume of the mixture used in each test was around 40 mL, and the separation took place within a few seconds. After the separation, the system was observed at rest for 5 to 10 min to check if any oil droplets permeated through the mesh. The oil−water separation efficiencies of all of the 12 combinations of oils and pore sizes are shown in Figure 5, along with the SEM images of the meshes used. The oil−water separation efficiency was calculated using the formula shown in eq 1.[24,25]

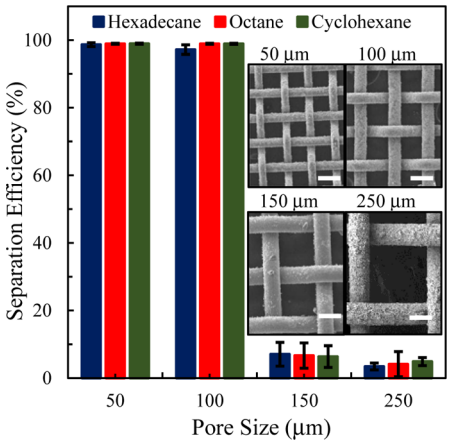

Figure 5. Measurement of the separation efficiency. Annealed TiO_2 coated mesh with four different pore sizes were used to separate oil–water mixtures. The scale bar in the SEM images is 100 μm.

$$\text{Eff} = \left(1 - \frac{C_p}{C_o}\right) \times 100\% \quad (1)$$

where C_o and C_p are the volume/volume ratios (v/v) of the original oil–water mixture and the filtered permeate, respectively. C_o and C_p were determined by measuring the volume ratio of oil with respect to the mixture (oil and water) using a graduated cylinder. The value of C_o used was 49 ± 6%. From Figure 5, it is clear that the annealed TiO_2 coated stainless steel mesh of 50 and 100 μm achieved 99% oil–water separation efficiency and a very small trace of oil was found in the permeate (water). However, the TiO_2 coated stainless steel meshes of higher pore size showed poor oil–water separation efficiency. It is clear from this study that a spray coating on the 100 μm stainless steel mesh (contrary to traditional cumbersome coating procedures) can be applied very effectively for the oil–water separation. More viscous or heavier oil such as hexadecane and relatively lower viscosity (or "lighter") oils like cyclohexane were tested for oil–water separation efficiencies. We found that the separation ability is independent of the viscosity of the oil. However, the rate of permeation did decrease when more viscous oils were tested.

DISCUSSION

The contact angle of oil droplet on a flat solid surface in water can be expressed using the Young–Dupré equation,[34] as written in eq 2:

$$\cos\theta_{ow} = \frac{\gamma_{sw} - \gamma_{so}}{\gamma_{ow}} = \frac{\gamma_{oa}\cos\theta_{oa} - \gamma_{wa}\cos\theta_{wa}}{\gamma_{ow}} \quad (2)$$

where γ_{sw} and γ_{so} are respectively solid/water and solid/oil interfacial tensions while γ_{oa}, γ_{wa}, and γ_{ow} are the surface tension of oil, surface tension of water, and the interfacial tension of an oil–water interface, respectively. The value of θ_{ow} becomes high when $\gamma_{wa}\cos\theta_{wa}$ is greater than the term $\gamma_{oa}\cos\theta_{oa}$. Thus, underwater–oil repellency can be increased by increasing the hydrophilicity of the immersed solid surface.[35] The surface morphology and the roughness of the surface can also increase the oil repellency as the surface texture traps pockets of water. This condition can be explained with the help of the Cassie–Baxter equation:[36,37]

$$\cos\theta_{ow}^{CB} = r_f f\cos\theta_{ow} + f - 1 \quad (3)$$

where r_f is the ratio of the real contact line to the projected contact line of the portion of solid that is in contact with the oil and f is the fraction of length of the projected area of the solid surface in contact with oil. Therefore, from eq 3, it is obvious that the surface treatment and surface texturing are important to achieve underwater superoleophobicity.

It is clear that the underwater superoleophobicity is an important factor for the oil–water separation process, but it is also apparent from our results in Figure 4 that it is not a sufficient criterion for oil–water separation and that surface roughness is also a governing factor in the oil–water separation process. As discussed earlier in the context of image 6 in Figure 2, underwater superoleophobicity can be achieved simply by annealing a stainless steel mesh, and it has been reported that even a clean glass slide also possesses superhydrophilicity and underwater–oil repellency.[38] It is evident from Figure 4a, that even though the annealed mesh exhibits underwater superoleophobicity, it failed in the oil–water separation. On the other hand, stainless steel meshes of same pore sizes (50 and 100 μm), when coated with TiO_2, showed 99% efficiency in oil–water separation, confirming that superhydrophilicity and underwater–oil repellency alone are not the sufficient conditions for oil–water separation

It can be seen from the SEM images of Figure 4b that, compared to the smooth annealed stainless steel surface, the TiO_2 coated mesh shows both micro and nanoscale roughness and this surface roughness contributes favorably for oil–water separation due to its increased underwater–oil repellency. Since annealed stainless steel is hydrophilic, the smooth surface is more favorably in contact with water, and this leads to high oil repellency. Defects on the solid surface can introduce pinning points that impact droplet mobility across the texture. Introducing a rough porous coating to the surface by covering it with TiO_2 nanoparticles enables this superhydrophilic texture to trap water within the roughness.[23] In addition to this, the strong affinity of TiO_2 toward water molecules can create a surface-adsorbed water layer such that an oil droplet is not at all in contact with the liquid impregnated surface, which is confirmed by the low values of sliding angle, that are exhibited by TiO_2 coated glass and TiO_2 coated stainless steel mesh.

Since the TiO_2 surface is also wettable by oil, the TiO_2 coated mesh must be prewetted by water before using it for oil–water separation. The presence of an adsorbed water layer on the porous TiO_2 surface is an important factor for oil–water separation. This adsorbed water layer plays two distinct roles in oil–water separation: first, it prevents oil droplets from coming into contact with the mesh during the separation process; second, this layer provides channels for the water droplets from the oil–water mixture to permeate to the opposite side of the coated mesh. These necessary conditions for oil–water separation cannot be met by annealed stainless steel mesh due to its smooth surface texture, the low affinity toward water molecules, and the presence of pinning defects that trap oil droplet on the surface leading to fouling.

Another factor which plays major role in oil–water separation is the pore size of the mesh. We observed that oil–water separation did not yield a desirable result when the pore size of the stainless steel mesh is greater than 100 μm. However, if an oil droplet is carefully placed on top of the TiO_2 coated mesh, the porous mesh can withstand the hydrostatic pressure of the oil column (see Figure S4). At a certain critical height, h_{max}, the oil starts flowing downward and penetrating the TiO_2 coated mesh. The intrusion pressure is expressed as a

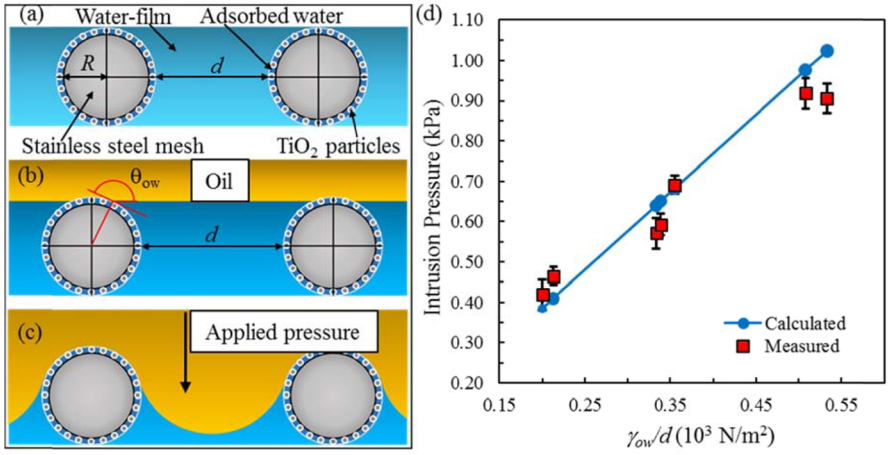

Figure 6. Intrusion pressure and illustrated configuration of oil–water meniscus. (a) The formation of a water film in the pore of the mesh. (b) Contact line of oil and water in equilibrium state. (c) The contact line of oil and water under applied pressure. (d) Comparison of measured and calculated result of the intrusion pressure.

hydrostatic head, $P_{int} = \rho g h_{max}$, where ρ is the density of oil and therefore P_{int} can be calculated by measuring the height, h_{max}. As the hydrostatic pressure falls below the intrusion pressure, i.e., after $h < h_{max}$, it is expected that the oil will stop flowing. Surprisingly, we find that once the oil starts flowing, it in fact keeps flowing until most of the oil phase is transferred to the other side of the mesh (see the video in the Supporting Information).

The formation of a water-film (capillary bridge) between the individual wires of the mesh is quite normal, because the pore size of the mesh is much smaller than the capillary length of water.[39,40] This contiguous water film is found to be one of the most important factors that govern the oil–water separation. In view of this fact, we develop a simple model for the contact line of oil, water, and solid interfaces in the TiO_2 coated mesh. Figure 6a shows the formation of a uniform water film between the two wires of the mesh, separated by a distance d (pore size of the mesh). When this prewetted mesh is in contact with oil, the three phase contact line adjusts in order to maintain the required underwater–oil contact angle, θ_{ow},[36,37] as illustrated in Figure 6b. From this, the intrusion pressure can be calculated using the Young–Laplace equation, given in eq 4.[24,41−43]

$$P_{int} = -\frac{2\gamma_{ow}\cos\theta_{ow}}{d} \tag{4}$$

This intrusion pressure is the excess pressure required in the oil phase to overcome the interfacial tension at the interface. At the critical condition, the vertical components of forces are balanced, $\Sigma F_y = F_P + F_\gamma = 0$, where F_P and F_γ are the force from external pressure and the force from the interfacial tension, respectively.[14,42] This force balance can be established only if θ_{ow} is larger than 90° so that the vertical components of F_P and F_γ are pointing in opposite directions. On the other hand, if θ_{ow} is less than 90°, there is no static force balance possible as F_P and F_γ are pointing in the same direction. The positive value of P_{int} (when $\theta_{ow} > 90°$) indicates that a hydrostatic pressure must be established in order to force the oil droplets into the mesh pores. Conversely, negative value of P_{int} (when $\theta_{ow} < 90°$) indicate that the oil phase needs no external pressure to spontaneously penetrate through the mesh pores.

The contact line illustrated in Figure 6c shows the situation when the system is under an applied pressure. If the applied pressure is greater than the intrusion pressure, the oil phase will break the water film, resulting in a change in the shape of the interfacial line, and under this condition, eq 4 is no longer valid to describe the system. Consequently, γ_{ow} and θ_{ow} need to be substituted by γ_{oa} and θ_{oa} respectively as the interface changed, where θ_{oa} is the contact angle of oil on water in air environment. The value of θ_{oa} can be calculated using the Young equation shown in eq 5.[39]

$$\cos\theta_{oa} = \frac{\gamma_{wa} - \gamma_{ow}}{\gamma_{oa}} \tag{5}$$

Numerical values for most of these parameters can be found in the literature.[44] Since γ_{wa} is generally larger than γ_{ow}, the value of $\cos\theta_{oa}$ is always positive. As a result, the intrusion pressure will have negative values and the oil phase will spontaneously channel down through the mesh. This is why we observed that the oil did not stop flowing after initial breakthrough is achieved, even when the hydrostatic pressure is reduced below the critical intrusion pressure.

Figure 6d depicts the plot of intrusion pressure versus γ_{ow}/d. The measured value was determined by measuring the maximum hydrostatic pressure discussed earlier and the calculated value was obtained using eq 4. Figure 6d indicates that the experimental value is statistically in agreement with the theoretical value. This result is important for selection of the correct pore size of mesh for oil–water separation. It is clear from eq 4 that the bigger the pore size, the smaller the intrusion pressure. If the intrusion pressure is small, the separation may fail as the impact force of the mixture fluctuates during the separation process.

CONCLUSION

We have demonstrated that superhydrophilic porous meshes with underwater–oil repellency for the application of oil–water separation can be easily fabricated by spray coating nanostructured particles onto stainless steel meshes of various sizes. A notable 99% oil–water separation efficiency was achieved using the coated mesh of pore sizes 50 and 100 μm, compared to no separation, found in the case of uncoated mesh of the same material and pore sizes. We also showed that establishing structures with underwater superoleophobicity is not sufficient to meet the conditions that lead to oil–water separation, i.e.,

the ability to steadily pass water through the coated mesh without permeating oil. Establishing a contiguous water-film between the pores of the mesh determines the capacity of the coated mesh to perform oil–water separation. The formation of such a water-film is promoted by three important factors: (i) the underwater superhydrophilicity of the surface of the mesh, (ii) the surface roughness of the microporous texture, and (iii) sufficiently small pore size of the mesh. These three factors control the stability and robustness of the contiguous water film that must exist in the porous filtration medium to ensure uninterrupted oil–water separation.

■ ASSOCIATED CONTENT

Supporting Information

Experimental setup, sliding angle measurements for uncoated and TiO_2 coated meshes, intrusion pressure measurements, and videos for oil–water separation. This material is available free of charge via the Internet at http://pubs.acs.org.

■ AUTHOR INFORMATION

Corresponding Author

*E-mail: magondal@kfupm.edu.sa. Tel: +966138602351. Fax: +966138602293.

Author Contributions

M.A.G. and M.A.D. contributed in design of concept and experimental setup, analysis of results and discussions, outlined and reviewed the manuscript. M.S.S. performed the experiments, collected data, and also contributed in drafting the manuscript. G.H.M., K.K.V., and D.P. contributed positively to technique development, analysis of results and discussions, and commented on manuscript drafts.

Notes

The authors declare no competing financial interest.

■ ACKNOWLEDGMENTS

The support of this work by KFUPM through Project Nos. MIT11109 and MIT11110 under the Center of Excellence for Scientific Collaboration with MIT is gratefully acknowledged. The support of the Physics Department of KFUPM is also acknowledged.

■ ABBREVIATIONS

CA, contact angle; SA, sliding angle; THF, tetrahydrofuran; IPA, isopropyl alcohol

■ REFERENCES

(1) Neff, J. M. *Bioaccumulation in Marine Organisms: Effects of Contaminants from Oil Well Produced Water*; Elsevier Science Publisher: Amsterdam, 2002.

(2) Veil, J. A.; Puder, M. G.; Elcock, D.; Redweik, R. J. *A White Paper Describing Produced Water from Production of Crude Oil, Natural Gas, and Coal Bed Methane*; US Department of Energy: Washington, DC, 2004.

(3) Fakhru'l-Razi, A.; Pendashteh, A.; Abdullah, L. C.; Biak, D. R. A.; Madaeni, S. S.; Abidin, Z. Z. Review of Technologies for Oil and Gas Produced Water Treatment. *J. Hazard. Mater.* **2009**, *170*, 530–551.

(4) Bailey, B.; Crabtree, M.; Tyrie, J.; Elphick, J.; Kuchuk, F.; Romano, C.; Roodhart, L. Water Control. *Oilfield Rev.* **2000**, *12*, 30–51.

(5) Fingas, M. *Oil Spill Science and Technology*; Elsevier Science Publisher: Amsterdam, 2011.

(6) Osamor, F. A.; Ahlert, R. C. *Oil/Water Separation: State of the Art*; U.S. Environmental Protection Agency: Cincinnati, 1978.

(7) Zhou, X.; Zhang, Z.; Xu, X.; Men, X.; Zhu, X. Facile Fabrication of Superhydrophobic Sponge with Selective Absorption and Collection of Oil from Water. *Ind. Eng. Chem. Res.* **2013**, *52*, 9411–9416.

(8) Zhu, Q.; Pan, Q.; Liu, F. Facile Removal and Collection of Oils from Water Surfaces through Superhydrophobic and Superoleophilic Sponges. *J. Phys. Chem. C* **2011**, *115*, 17464–17470.

(9) Feng, L.; Zhang, Z.; Mai, Z.; Ma, Y.; Liu, B.; Jiang, L.; Zhu, D. A Super-hydrophobic and Super-oleophilic Coating Mesh Film for the Separation of Oil and Water. *Angew. Chem., Int. Ed.* **2004**, *43*, 2012–2014.

(10) Wang, B.; Guo, Z. Superhydrophobic Copper Mesh Films with Rapid Oil/Water Separation Properties by Electrochemical Deposition Inspired from Butterfly Wing. *Appl. Phys. Lett.* **2013**, *103*, 063704.

(11) Yang, J.; Zhang, Z.; Xu, X.; Zhu, X.; Men, X.; Zhou, X. Superhydrophilic-Superoleophobic Coatings. *J. Mater. Chem.* **2012**, *22*, 2834–2837.

(12) Hu, B.; Scott, K. Influence of Membrane Material and Corrugation and Process Conditions on Emulsion Microfiltration. *J. Membr. Sci.* **2007**, *294*, 30–39.

(13) Maartens, A.; Jacobs, E. P.; Swart, P. UF of Pulp and Paper Effluent: Membrane Fouling-Prevention and Cleaning. *J. Membr. Sci.* **2002**, *209*, 81–92.

(14) Kwon, G.; Kota, A. K.; Li, Y.; Sohani, A.; Mabry, J. M.; Tuteja, A. On-Demand Separation of Oil-Water Mixtures. *Adv. Mater.* **2012**, *24*, 3666–3671.

(15) Zhang, L.; Zhang, Z.; Wang, P. Smart Surfaces with Switchable Superoleophilicity and Superoleophobicity in Aqueous Media: Toward Controllable Oil/Water Separation. *NPG Asia Mater.* **2012**, *4*, 1–8.

(16) Kota, A. K.; Kwon, G.; Choi, W.; Mabry, J. M.; Tuteja, A. Hygro-Responsive Membranes for Effective Oil-Water Separation. *Nat. Commun.* **2012**, *3*, 1025.

(17) Tuteja, A.; Choi, W.; Ma, M.; Mabry, J. M.; Mazzella, S. A.; Rutledge, G. C.; Cohen, R. E. Designing Superoleophobic Surfaces. *Science* **2007**, *318*, 1618–1622.

(18) Cao, L.; Price, T. P.; Weiss, M.; Gao, D. Super Water- and Oil-Repellent Surfaces on Intrinsically Hydrophilic and Oleophilic Porous Silicon Films. *Langmuir* **2008**, *24*, 1640–1643.

(19) Zhang, M.; Zhang, T.; Cui, T. Wettability Conversion from Superoleophobic to Superhydrophilic on Titania/Single-Walled Carbon Nanotube Composite Coatings. *Langmuir* **2011**, *27*, 9295–9301.

(20) Cassie, A. B. D.; Baxter, S. Wettability of Porous Surfaces. *Trans. Faraday Soc.* **1944**, *40*, 546–551.

(21) Wenzel, R. N. Surface Roughness and Contact Angle. *J. Phys. Colloid Chem.* **1949**, *53*, 1466–1467.

(22) Zhang, L.; Zhong, Y.; Cha, D.; Wang, P. A Self-Cleaning Underwater Superoleophobic Mesh for Oil-Water Separation. *Sci. Rep.* **2013**, *3*, 2326.

(23) Sawai, Y.; Nishimoto, S.; Kameshima, Y.; Fujii, E.; Miyake, M. Photoinduced Underwater Superoleophobicity of TiO2 Thin Films. *Langmuir* **2013**, *29*, 6784–6789.

(24) Xue, Z.; Wang, S.; Lin, L.; Chen, L.; Liu, M.; Feng, L.; Jiang, L. A Novel Superhydrophilic and Underwater Superoleophobic Hydrogel-Coated Mesh for Oil/Water Separation. *Adv. Mater.* **2011**, *23*, 4270–4273.

(25) Tian, D.; Zhang, X.; Tian, Y.; Wu, Y.; Wang, X.; Zhai, J.; Jiang, L. Photo-Induced Water-Oil Separation Based on Switchable Superhydrophobicity- Superhydrophilicity and Underwater Superoleophobicity of the Aligned ZnO Nanorod Array-Coated Mesh Films. *J. Mater. Chem.* **2012**, *22*, 19652–19657.

(26) Chen, Y.; Xue, Z.; Liu, N.; Lu, F.; Cao, Y.; Sun, Z.; Feng, L. Fabrication of a Silica Gel Coated Quartz Fiber Mesh for Oil-Water Separation Under Strong Acidic and Concentrated Salt Conditions. *R. Soc. Chem. Adv.* **2014**, *4*, 11447–11450.

(27) Zeng, J.; Guo, Z. Superhydrophilic and Underwater Superoleophobic MFI Zeolite-Coated Film for Oil/Water Separation. *Colloids Surf., A* **2014**, *444*, 283–288.

(28) Srinivasan, S.; Chhatre, S. S.; Mabry, J. M.; Cohen, R. E.; McKinley, G. H. Solution Spraying of Poly(methyl methacrylate) Blends to Fabricate Microtextured, Superoleophobic Surfaces. *Polymer* **2011**, *52*, 3209−3218.
(29) Ogihara, H.; Xie, J.; Saji, T. Factors Determining Wettability of Superhydrophobic Paper Prepared by Spraying Nanoparticle Suspensions. *Colloids Surf., A* **2013**, *434*, 35−41.
(30) Halpegamage, S.; Tao, J.; Kramer, A.; Sutter, E.; Batzill, M. Why Is Anatase a Better Photocatalyst Than Rutile? - Model Studies on Epitaxial TiO2 Films. *Sci. Rep.* **2013**, *4*, 4043.
(31) Gondal, M. A.; Sadullah, M. S.; McKinley, G. H.; Varanasi, K. K.; Panchanathan, D. Photo-Induced In Situ Switching of Surface Wettability of Titania Films Under Air and Oil Environment. *HONET-CNS 2013* **2013**, 151−154.
(32) Tian, Y.; Jiang, L. Wetting: Intrinsically Robust Hydrophobicity. *Nat. Mater.* **2013**, *12*, 291−292.
(33) Takeda, S.; Fukawa, M. Surface OH Groups Governing Surface Chemical Properties of SiO2 Thin Films Deposited by RF Magnetron Sputtering. *Thin Solid Films.* **2003**, *444*, 153−157.
(34) Good, R. J. Contact Angle, Wetting, and Adhesion: a Critical Review. *J. Adhes. Sci. Technol.* **1992**, *6*, 3−36.
(35) Jung, Y. C.; Bhushan, B. Wetting Behavior of Water and Oil Droplets in Three-Phase Interfaces for Hydrophobicity/Philicity and Oleophobicity/Philicity. *Langmuir* **2009**, *25*, 14165−14173.
(36) Kawase, T.; Fujii, T.; Minagawa, M. Repellency of Textile Assemblies. Part I: Apparent Contact Angle of Wax-Coated Monofilament Mesh Screen. *Text. Res. J.* **1987**, *57*, 185−191.
(37) Michielsen, S.; Lee, H. J. Design of a Superhydrophobic Surface Using Woven Structures. *Langmuir* **2007**, *23*, 6004−6010.
(38) Grate, J. W.; Dehoff, K. J.; Warner, M. G.; Pittman, J. W.; Wietsma, T. W.; Zhang, C.; Oostrom, M. Correlation of Oil-Water and Air-Water Contact Angles of Diverse Silanized Surfaces and Relationship to Fluid Interfacial Tensions. *Langmuir* **2012**, *28*, 7182−7188.
(39) Good, R. J.; Islam, M. Liquid Bridges and the Oil Agglomeration Method of Coal Beneficiation: An Elementary Theory of Stability. *Langmuir* **1991**, *7*, 3219−3221.
(40) Chen, T. Y.; Tsamopoulos, J. A.; Good, R. J. Capillary Bridges between Parallel and Non-Parallel Surfaces and Their Stability. *J. Colloid Interface Sci.* **1992**, *151*, 49−69.
(41) Lafuma, A.; Quéré, D. Superhydrophobic States. *Nat. Mater.* **2003**, *2*, 457−460.
(42) Chen, P.; Xu, Z. Mineral-Coated Polymer Membranes with Superhydrophilicity and Underwater Superoleophobicity for Effective Oil/Water Separation. *Sci. Rep.* **2013**, *3*, 2776.
(43) Journet, C.; Moulinet, S.; Ybert, C.; Purcell, S. T.; Bocquet, L. Contact Angle Measurements on Superhydrophobic Carbon Nanotube Forests: Effect of Fluid Pressure. *Europhys. Lett.* **2005**, *71*, 104−109.
(44) Yoon, H.; Oostrom, M.; Werth, C. J. Estimation of Interfacial Tension between Organic Liquid Mixtures and Water. *Environ. Sci. Technol.* **2009**, *43*, 7754−7761.